

# **An artificial bee colony optimization based matching pursuit approach for ultrasonic echo estimation**

*Ai-Ling Qi<sup>1</sup>, Guang-Ming Zhang<sup>2\*</sup>, Ming Dong<sup>3</sup>, Hong-Wei Ma<sup>3</sup>, David M Harvey<sup>2</sup>,*

<sup>1</sup>School of Computer Science and Technology, Xi'an University of Science and Technology,  
Yanta Road 58, Xi'an Shaanxi, 710054, China

<sup>2</sup>General Engineering Research Institute, Liverpool John Moores University, Byrom Street,  
Liverpool, L3 3AF, United Kingdom

<sup>3</sup>School of Mechanical Engineering, Xi'an University of Science and Technology, Xi'an,  
710054, China

\* Corresponding author. Tel: +44-1512312113; E-mail: g.zhang@ljmu.ac.uk.

## **Highlights**

- Proposed a modified matching pursuit approach.
- Artificial bee colony optimization is integrated into the matching pursuit approach.
- Search optimal atoms in a continuous parameter space of atoms.
- High accuracy of ultrasonic echo estimation.

## **Abstract**

Ultrasonic echo estimation is important in ultrasonic non-destructive evaluation and material characterization. Matching pursuit is one of the most popular methods for the purpose of estimating ultrasonic echoes. In this paper, an artificial bee colony optimization based matching pursuit approach (ABC-MP) is proposed specifically for ultrasonic signal decomposition by integrating the artificial bee colony algorithm into the matching pursuit method. The optimal atoms are searched from a continuous parameter space over a tailored Gabor dictionary in ABC-MP instead of a discrete parameter space in matching pursuit. As a result, echoes characterized by a set of physical parameters can be estimated accurately and efficiently. The performance of ABC-MP is tested using both simulated signals and real ultrasonic signals, and compared with matching pursuit. Results clearly demonstrate the superior performance of the proposed ABC-MP approach over matching pursuit in ultrasonic echo estimation in terms of the shape and amplitude of the recovered echoes and the reconstructed signal, and the residue signal.

**Keywords:** Artificial bee colony optimization; Matching pursuit; Gabor dictionary; Sparse signal representation; Ultrasonic echo estimation;

## 1. Introduction

### 1.1 Modelling of ultrasonic signals

Ultrasonic inspection is one of the most widely used techniques for non-destructive evaluation (NDE) of materials, and its applications in industries range from defect detection, structural health monitoring, and measurement of material properties. In ultrasonic NDE, an ultrasonic transducer sends pulses and receives reflected echoes from discontinuities in the test sample. According to the acoustic propagation theory, a reflected ultrasonic echo  $s(t)$  from a flat surface reflector in pulse-echo mode ultrasonic inspection is often modelled approximately [1] as

$$s(t) = c \exp(-B_\alpha(t - \tau)^2) \cos(2\pi f_c(t - \tau) + \varphi). \quad (1)$$

Let  $\theta = [c, B_\alpha, f_c, \tau, \varphi]$  denote the parameter vector. The parameters of this model are closely related to the physical properties of the ultrasonic signal propagating through the material. The amplitude of the echo  $c$  is primarily governed by the acoustic impedance values of the materials involved, the attenuation of the original signal, and the size and orientation of the reflector. The parameters  $B_\alpha$  and  $f_c$  are the bandwidth factor and centre frequency, respectively. These parameters are governed by the transducer frequency characteristics and the propagation path. The time of flight  $\tau$  is related to location of the reflector as the distance between the transducer and the reflector. The phase of the echo  $\varphi$  accounts for the distance, acoustic impedance, size, and orientation of the reflector. Therefore, ultrasonic echoes reflected from homogeneities or discontinuities in tested samples contain information pertaining to the location, size, and characteristics of defects, along with the material and

geometry of the test sample [2].

For pulse-echo mode ultrasonic inspection, a recorded signal  $y(t)$  is a superposition of ultrasonic echoes  $s_i(t)$  reflected from different interfaces inside the test sample,

$$y(t) = \sum_{i=1}^m s_i(t) + \xi(t), \quad (2)$$

where  $\xi(t)$  accounts for the noise originating from the measurement system and materials.

Equation (2) can be further expanded as:

$$y(t) = \sum_{i=1}^m c_i \phi_i(t) + \xi(t), \quad (3)$$

where  $\phi_i(t)$  is the incident pulse impinged to the  $i^{\text{th}}$  interface, and  $c_i$  are the reflection coefficients. Due to the limited interfaces and defects in the test sample, the reflection coefficients  $c_i$  are generally a sparse distribution. From Equation (3), it can be seen that ultrasonic echo estimation can be formulated as the problem of blind source separation that separates a set of linear mixtures into a number of unknown source signals, inferring both the reflection coefficients  $c_i$ , which can be considered as the virtual ultrasonic sources, and the ultrasonic incident pulses  $\phi_i(t)$  from the observed signal  $y(t)$ .

## ***1.2 Ultrasonic echo estimation via sparse signal representation***

From Section 1.1, it can be seen that the accurate detection, location and sizing of defects during ultrasonic inspection are limited by the ability to precisely estimate the information of the reflected echoes contained in the recorded ultrasonic signals, including amplitudes/reflection coefficient, time positions, and shape of the echoes. Therefore, ultrasonic echo estimation is an important issue in ultrasonic NDE. Various signal processing techniques have been developed to tackle this issue, and a review can be found in Ref. [3].

The most appealing method among them is sparse signal representation (SSR), an emerging signal processing technique.

SSR decomposes a signal over an overcomplete dictionary. Assume that a dictionary  $D = \{\phi_i\}_{i=1}^L$  consists of  $L$  atoms  $\phi_i$ . The atoms are  $N$ -dimensional with unit norm, that is,  $\phi_i \in R^N$  and  $\|\phi_i\|_2 = 1$ .  $N < L$  so that  $D$  is overcomplete. For a given signal  $y \in R^N$ , the SSR technique is to seek a sparse vector  $c \in R^L$  satisfying the relationship:

$$y = Dc + \varepsilon, \quad (4)$$

where  $\varepsilon$  is an error term. This corresponds to solving the following variational problem: Minimize  $\|c\|_0$  subject to  $y = Dc$ , where  $\|\cdot\|_0$  is the  $L^0$ -norm, counting the non-zero entries of a vector. Directly solving the sparse decomposition problem is NP-hard. The existing SSR algorithms are commonly developed by simplifying the NP-hard problem as a constrained optimization problem by greedy approximations or by applying  $L^1$ -norm or  $L^p$ -norm constraints on the decomposition coefficients to find sub-optimal solutions. Many SSR algorithms have been developed in the past two decade, such as matching pursuit (MP) [4], greedy basis pursuit [5], Sparse Bayesian learning (SBL) [6], nonconvex regularization [7], and applications of SSR extend into many fields [8-12].

Comparing Equations (3) and (4), it can be seen that ultrasonic echo estimation problem can be addressed by SSR directly. Through the sparse decomposition of an observed signal  $y(t)$ , both the reflection coefficients  $c_i$  and the ultrasonic echoes  $\phi_i(t)$  can be estimated. Although under an overcomplete dictionary the decomposition of a signal is underdetermined, recent research shows that in many applications this can offer great advantages compared to the conventional signal processing methods. One is that there is greater flexibility in

capturing structure in the data [13]. Instead of a small set of general basis vectors, there is a larger set of more specialized atoms such that relatively few are required to represent any particular signal. The second is super-resolution [14]. We can obtain a resolution of sparse objects that is much higher than that possible with traditional methods. The third is that overcomplete representations increase stability of the representation in response to small perturbations of the signal. The fourth is that the redundant representations have the desired shift invariance property [15]. These advantages of SSR are of benefit to the interpretation of an ultrasonic signal. In the past decade, research on SSR in the community of ultrasonic NDE signal processing has attracted an increasing interest and become a hot research area. In [16], MP was used to extract ultrasonic wave shape features of debris echoes and air bubble echoes, and by utilizing the extracted wave shape features, the debris with different shapes and air bubble are distinguished. In [17], SBL was used to denoise the guided wave signal for damage detection. In [18], SBL was employed to estimate the range of frequency and bandwidth parameters of the flaw echoes for structure noise elimination and flaw detection. In [19], taking the advantages of accurate echo separation and echo estimation, MP was integrated into a conventional acoustic micro imaging system, resulting in a super-resolution imaging method. In [20], MP is implemented by the selection of a coarse set of atoms in a tailored discrete Gabor dictionary and interpolation of the atom parameters to improve the accuracy of ultrasonic echo estimation. A comprehensive review about the existing SSR algorithms and their applications in ultrasonic NDE can be found in our recent paper of Ref.[21]. Among all the SSR algorithms, MP is one of the most popular algorithms used in ultrasonic NDE for ultrasonic echo estimation.

### 1.3 Problem statement

It has been shown that the behavior of the overcomplete dictionary has a great impact on the performance of the SSR methods [22]. In ultrasonic NDE, an ultrasonic echo is usually a broadband pulse modulated at the centre frequency of the transducer, and is usually modelled as a Gabor function as described in Equation (1). Therefore, the discrete Gabor dictionary is normally used in SSR of ultrasonic signals.

The real Gabor dictionary is defined by  $D_R = \{g_{(\gamma,w)}: (\gamma,w) \in \Gamma \times [0, 2\pi]\}$  [23], where  $\gamma = (s, u, v)$ . For convenience we use the notation  $\beta = (\gamma, w)$ .  $g_\beta$  is Gabor atoms:

$$g_\beta = g_{(\gamma,w)} = \frac{K_\gamma}{\sqrt{s}} g\left(\frac{t-u}{s}\right) \cos(vt+w), \quad (5)$$

where:  $s$  is the scale of the function,  $u$  its translation,  $v$  its frequency modulation, window function  $g(t)$  is Gaussian function  $g(t) = e^{-\pi^2 t^2}$ , constant and factor  $\frac{K_\gamma}{\sqrt{s}}$  normalizes  $g_\beta$ , and  $w$  is the phase of the real Gabor atoms.

In practical applications, signal decomposition is normally performed in the discrete Gabor dictionary  $D_\alpha = \{g_\beta: \beta \in \Gamma_\alpha \times [0, 2\pi]\}$ , a subset of  $D_R$ , where  $\Gamma_\alpha$  is composed of all  $\gamma = (a^j, pa^j \Delta u, ka^{-j} \Delta v)$  with  $\Delta u = \frac{\Delta v}{2\pi}$  and  $\Delta u \cdot \Delta v < 2\pi$ ,  $j \in \mathbb{Z}, p \in \mathbb{Z}, k \in \mathbb{Z}$  [24]. In the practical sparse decomposition, the parameters  $\gamma = (s, u, v)$  are normally discretised as follows:

- $s[j] = a^j$ , for  $1 \ll j \ll n$  where  $n$  is the biggest integer power of  $a$  such that  $a^n \leq N$ , where  $N$  is the length of the input signal. In many applications,  $a$  is set as 2.
- $du[j] = s[j]/2$  and  $dv[j] = \pi/s[j]$ .
- $u \in \{pdu | p \in \mathbb{Z}, 0 \leq pdu \leq n-1\}$ .

- $v \in \{kdv | k \in \mathbb{Z}, 0 \leq kdv < rmv\}$ , where  $rmv = 2\pi$ .

It is proven in [23, 24] that if the parameters  $s, u, v$  are discretised as indicated above the fourth parameter  $w$  is uniquely determined in the standard MP algorithm.

In our application, the atoms in the overcomplete dictionary should match the ultrasonic echoes as close as possible in order to obtain accurate echo estimation. In order to achieve this goal, the parameters  $s, u, v$  in the real Gabor dictionary  $D_R$  is required to be discretised as fine as possible rather than the above partition. In [20], it demonstrated that refining the parameters significantly improves the performance of MP.

However, for given parameter bounds, this means significantly increase the size of the discrete Gabor dictionary  $D_\alpha$ . According to the SSR theory, MP finds the optimal solution only when the dictionary size, i.e., the number of atoms in the dictionary, is smaller than a threshold due to cumulative coherence bound [22]. Otherwise MP fails to find the optimal solution, and the decomposition is not stable and reliable as well.

This contradiction is caused by the greedy searching strategy when MP searches for the best matching atoms over an overcomplete dictionary iteratively. Because of its greediness, MP initially may select an atom that is not part of the optimal sparse representation; as a result, many of the subsequent atoms selected by MP simply compensate for the poor initial selection.

One solution to this problem is to refine the resolution of the parameter space by improving the search from a coarse grid to a fine grid and then interpolating both the fine grid and the time shift parameter [20]. This strategy significantly improves the MP performance without increasing the size of the dictionary.



In this paper an alternative solution to this problem is proposed. The greedy searching method in MP is replaced by a search method that is able to find the global solution in a continuous parameter space of atoms. This replacement is assumed to significantly alleviate the above contradiction and achieve high performance for ultrasonic echo estimation although it may not be able to completely eliminate the drawbacks of MP. Many optimization algorithms might be used to realize this idea, for example particle swarm optimization [25], simulated annealing [26], and artificial bee colony algorithm (ABC) [27-29]. Without loss of generality, ABC is used in this paper to test this idea because ABC can find the global optimal solution with quick convergence by carrying out a parallel global searching in a continuous parameter space.

The rest of the paper is organized as follows. Section 2 presents a brief review of the MP and ABC algorithms. This will facilitate the description of the proposed algorithm. In Section 3, an ABC optimization based MP approach (ABC-MP) is proposed and detailed numerical implementation is presented. Experimental verification and performance analysis are given in Section 4. Finally, we conclude in Section 5.

## **2. Review of the MP algorithm and ABC algorithm**

### ***2.1 Review of the MP algorithm***

MP computes a signal representation by greedily constructing successive approximations to the signal,  $y^{(0)}$ ,  $y^{(1)}$ ,  $y^{(2)}$ ,  $\dots$ , by orthogonal projections on atoms of the dictionary  $D_\alpha$ . The following summarizes the steps of the MP algorithm [24]:

1) Initialize the iteration counter  $k = 1$ , the initial approximation  $y^{(0)} = 0$ , and the residue  $R^{(0)} = y$  where  $y$  is the measured ultrasonic signal.

2) Search the dictionary atom  $g_{\beta_k}$  that best correlates with the residue  $R^{(k-1)}$ .

This is achieved by solving the optimization problem:

$$g_{\beta_k} = \operatorname{argmax}_{g_{\beta} \in D_{\alpha}} \|\langle R^{(k-1)}, g_{\beta} \rangle\|. \quad (6)$$

3) Calculate a new approximation  $y^{(k)} = y^{(k-1)} + c_k g_{\beta_k}$  and a new residue  $R^{(k)} = y - y^{(k)}$ , where  $c_k$  is computed by the  $L^2$ -inner product of  $R^{(k-1)}$  and  $g_{\beta_k}$ , i.e.,

$$c_k = \langle R^{(k-1)}, g_{\beta_k} \rangle. \quad (7)$$

4) If the residue energy  $\|R^{(k)}\|_2 < \varepsilon$ , then stop. Otherwise  $k = k + 1$  and jump to Step 2.

After  $K$  iterations, matching pursuit decomposes the signal  $y$  into

$$y = \sum_{i=1}^K c_i g_{\beta_i} + R^{(K)}. \quad (8)$$

## 2.2 Review of the ABC algorithm

The ABC algorithm is an optimization algorithm evolved from the honey bees efficient behavior introduced by Karaboga [27]. In the ABC algorithm, the position of a nectar source represents a possible solution to the optimization problem and the nectar amount of a nectar source corresponds to the quality (fitness) of the associated solution. The number of the employed bees or the onlooker bees is equal to the number of solutions in the population. In the basic ABC algorithm, it firstly generates a population with  $S_N$  initial nectar source positions ( $S_N$  solutions) that are randomly distributed, where  $S_N$  denotes the number of nectar sources (the size of population). This can be done using Equation (9):

$$X_i = X_{low} + \operatorname{rand}(0,1) \times (X_{up} - X_{low}), \quad (i = 1, 2, \dots, S_N). \quad (9)$$

Each solution  $X_i$  is represented by a  $P$ -dimensional vector, where  $P$  is the number of the optimization parameters.  $X_{up}$  and  $X_{low}$  are the upper and lower bounds of these optimization parameters.  $\text{rand}(0,1)$  indicates a random number between 0 and 1.

After initialization, the nectar source positions (solutions) are then updated iteratively through the neighbourhood search processes of the employed bees, the onlooker bees and scout bees. An employed bee produces a modification on the position (solution) in her memory depending on the local information (visual information) and tests the nectar amount (fitness value) of the new source (new solution). Modification of the position is implemented by changing the parameters of the nectar position using Equation (10):

$$z_{ij} = x_{ij} + \varphi_{ij}(x_{ij} - x_{kj}), \quad i \in \{1, 2, \dots, S_N\}, \quad k \in \{1, 2, \dots, S_N\}, \quad j \in \{1, 2, \dots, P\}, \quad (10)$$

where  $x_{ij}$  is the current nectar source position,  $x_{kj}$  is a random nectar source position, and  $z_{ij}$  is the searched new nectar source position.  $\varphi_{ij}$  is a random number between  $[-1, 1]$ , and it controls the production of neighbor nectar sources around  $x_{ij}$ .  $k$  is a randomly chosen index, and  $k \neq i$ . In Equation (10), if a parameter value produced by this operation exceeds its predetermined limit, the parameter can be set to an acceptable value. Provided that the nectar amount of the new one is higher than that of the previous one, the bee memorizes the new position and forgets the old one. Otherwise she keeps the position of the previous one in her memory.

After all employed bees complete the searching process, they share the nectar information of the nectar sources and their position information with the onlooker bees on the dance area. An onlooker bee evaluates the nectar information taken from all employed bees and chooses a nectar source with a probability related to its nectar amount. The probability is

calculated using Equation (11) in this work:

$$p_i = \frac{Fit_i}{\sum_{n=1}^{S_N} Fit_n}, \quad (11)$$

where  $Fit_i$  is the fitness value of the nectar source  $X_i$ . As in the case of the employed bee, the onlooker bee produces a modification on the position in her memory and checks the nectar amount of the candidate source. Providing that its nectar is higher than that of the previous one, the bee memorizes the new position and forgets the old one.

If a nectar source has not updated when the preset iteration limit of abandonment is reached, this nectar source will be abandoned because it is likely to be a local optimum. The associated employed bee turns into a scout bee. The scout bee then discovers a new nectar source to replace the abandoned one. In the ABC algorithm, this is implemented by producing a random nectar source to replace the abandoned one using Equation (12):

$$x_{ij} = x_{low}^j + rand(0,1) \times (x_{up}^j - x_{low}^j), \quad (12)$$

where  $x_{low}^j = \min\{x_{1j}, x_{2j}, \dots, x_{S_N j}\}$ ,  $x_{up}^j = \max\{x_{1j}, x_{2j}, \dots, x_{S_N j}\}$ ,  $j \in \{1, 2, \dots, P\}$ . After the discovery operation, the scout bee turns back to be an employed bee.

After each candidate source position  $z_{ij}$  is produced and then evaluated by the artificial bee, its performance is compared with that of its old one. If the new food has equal or better nectar than the old source, it is replaced with the old one in the memory. Otherwise, the old one is retained in the memory. In other words, a greedy selection mechanism is employed as the selection operation between the old and the candidate one.

Repeat the above steps, until the maximum iteration number is reached or a convergence criterion is satisfied.

### 3. ABC optimization based MP

In this Section, the numerical implementation of the proposed ABC-MP approach is described in detail. The basic principle of ABC-MP is that, the optimization problem of Equation (6) in the standard MP algorithm is solved using the ABC algorithm in a continuous parameter space of atoms, instead of carrying out the greedy search in the discrete overcomplete dictionary  $D_\alpha$ .

#### 3.1 Interlink of ultrasonic echoes, Gabor atoms, and nectar sources

Since the ABC-MP algorithm is designed for ultrasonic echo estimation, an atom  $g_\beta$  represents an ultrasonic echo, and the decomposed coefficients in the ABC-MP decomposition of the ultrasonic signal correspond the ultrasonic reflection coefficients.

A nectar source in ABC-MP is an atom  $g_\beta$  so that each nectar source position  $X_i$  described in Section 2.2 is represented by the four parameters  $s, u, v, w$ , which will be optimized using the ABC algorithm. The physical meaning of the four parameters in ultrasonic NDE can be found in Section 1.1. The fitness value for a nectar source  $X_i$  is calculated as the inner product's absolute value of the ultrasonic signal  $y$  and the nectar source using the following equation:

$$Fit_i = \langle y, X_i \rangle. \quad (13)$$

The higher the fitness value, the better the nectar source, i.e., the better atom  $g_\beta$ . The fitness value of an atom corresponds the reflection coefficient of the found ultrasonic echo.

#### 3.2 Numerical implementation of the ABC-MP approach

The basic structure of ABC-MP is similar to MP, which computes a signal approximation by iteratively searching a global optimal ultrasonic echo from the residue signal,  $R^{(0)}$ ,  $R^{(1)}$ ,  $R^{(2)}$ , ...,  $R^{(m)}$ .  $m$  is the estimated number of ultrasonic echoes in the recorded ultrasonic NDE signal  $y$ .

The main steps of the ABC-MP algorithm are given below:

- 1) Initialization. Set the upper and lower bounds of the Gabor atom parameters  $\beta = (s, u, v, w)$ ; Set the initial approximation  $y^{(0)} = 0$ , and the residue signal  $R^{(0)} = y$  where  $y$  is the recorded ultrasonic signal.
- 2) Iteration  $k=1$
- 3) Repeat
- 4) Search the dictionary atom  $g_{\beta_k}$  that best correlates with the residue signal  $R^{(k-1)}$  from the continuous parameter space of Gabor atoms using the ABC algorithm.
- 5) Save the optimal atom  $g_{\beta_k}$  found at the iteration  $k$  by the ABC algorithm as a found ultrasonic echo in the residue signal  $R^{(k)}$ .
- 6) Save the fitness value  $c_k$  of the optimal atom  $g_{\beta_k}$  as the amplitude of the found ultrasonic echo in the residue signal  $R^{(k)}$ .
- 7) Calculate a new approximation and a new residue by  $y^{(k)} = y^{(k-1)} + c_k g_{\beta_k}$  and a new residue  $R^{(k)} = y - y^{(k)}$ .
- 8)  $k=k+1$
- 9) Until iteration  $k=m$ , or a convergence criterion is satisfied.

The reconstructed ultrasonic signal can then be approximated by:

$$y = \sum_{k=1}^m c_k g_{\beta_k} + R^{(m)}. \quad (14)$$

At iteration  $k$  and in the step 4 of ABC-MP, the search process is to solve the following optimization problem:

$$X_i = \operatorname{argmax}_{X_i \in D_R} \|\langle R^{(k-1)}, X_i \rangle\|. \quad (15)$$

A nectar source  $X_i$  is a Gabor atom  $g_\beta$ , which is defined by the four parameters  $\beta = (s, u, v, w)$ . The upper and lower bounds of the positions of the nectar sources, i.e., the bounds of  $D_R$ , are determined by the bounds of the parameters  $\beta$ .

The pseudo-code of the ABC algorithm used in the step 4 of the ABC-MP algorithm is given as below:

- 1) Initialize the population of solutions  $x_{ij}$ ,  $i = 1 \dots S_N$ ,  $j = 1 \dots 4$
- 2) Iteration=1
- 3) Repeat
- 4) Produce new solutions  $z_{ij}$  for the employed bees by using Equation (10) and evaluate them
- 5) Apply the greedy selection process as described in Section 2.2
- 6) Calculate the probability values  $p_{ij}$  for the solutions  $x_{ij}$  by using Equation (11)
- 7) Produce the new solutions  $z_{ij}$  for the onlookers from the solutions  $x_{ij}$  selected depending on  $p_{ij}$  and evaluate them
- 8) Apply the greedy selection process
- 9) Determine the abandoned solution for the scout bees, if exists, and replace it with a new randomly produced solution  $x_{ij}$  by using Equation (12)
- 10) Memorize the best solution achieved so far
- 11) iteration=iteration+1

12) Until iteration= the maximum iteration number.

13) Return the optimal  $x_{ij}$  as the found optimal atom  $g_{\beta_k}$  in the residue signal  $R^{(k)}$ , and the corresponding fitness value as the found  $c_k$ .

### ***3.4 Determination of the upper and lower bounds of the Gabor atom parameters***

In our practical applications, when an ultrasonic signal consists of multiple ultrasonic echoes that are heavily overlapped, it shows that the choices of the upper and lower bounds of the Gabor atom parameters have a significant impact on the stability and reliability of the ABC-MP algorithm. In this work, the following strategies are adopted to determine the upper and lower bounds of the Gabor atom parameters:

- The upper and lower bounds of the four parameters  $\beta = (s, u, v, w)$  are predetermined according to the a-prior information of the ultrasonic inspection system, including the characteristics of the used transducer and the attenuation properties of the test sample. During ultrasonic NDE, changing of the parameters  $s$  and  $v$  is mainly caused by the dispersive attenuation. High frequency has a high attenuation and low frequency has a low attenuation, as a result, leading to a frequency shift. The bound of  $s$  is estimated according to transducer bandwidth and the attenuation properties of the test sample. The bound of  $v$  is estimated based on the central frequency of the transducer and the attenuation properties of the test sample.  $u$  is between 0 to the length of the signal, and  $w$  is between 0 to  $2\pi$ .
- For a real ultrasonic echo with a high central frequency, it must have a relative small scale  $s$ . On the contrary, a low frequency ultrasonic echo has a relative large scale  $s$ .



On the basis of this physical property, when modifying the parameter  $\nu$  using the Equation (10) during the neighboring search process of the ABC algorithm, the parameter  $s$  will be checked so that the new nectar source (i.e, the new ultrasonic echo) has a clear physical interpretation. This is achieved by: during the modification of  $\nu$ , we firstly estimate the ideal parameter  $s$  according to the used transducer characteristics and the attenuation properties of the test sample, which is used as a reference  $s_c$ . Then, the parameter  $s$  of the new nectar source will be checked. If it is not in a reasonable range ( $s_1, s_2$ ) around  $s_c$ , the parameter  $s$  will be shift into this range.

- Similar to the above, when modifying the parameter  $s$ , the parameter  $\nu$  will be checked. This is achieved by: during the modification of  $s$ , we firstly estimate the ideal parameter  $\nu$  which is used as a reference  $\nu_c$ . Then, the parameter  $\nu$  will be checked if it is in a reasonable range ( $\nu_1, \nu_2$ ) around  $\nu_c$ . If not, the parameter  $\nu$  will be shift into this range.
- $s_1, s_2, \nu_1$  and  $\nu_2$  will be set empirically according to the given applications. If  $s_1$  and  $s_2$  are too close to  $s_c$ , and  $\nu_1$  and  $\nu_2$  are too close to  $\nu_c$ , it will affect the convergence of the ABC algorithm and even miss the optimal atoms because  $s_c$  and  $\nu_c$  are estimated. Obviously, if  $s_1$  and  $s_2$  are too deviated from  $s_c$ , and  $\nu_1$  and  $\nu_2$  are too deviated from  $\nu_c$ , it will lose the purpose of forcing the searched atom with a clear physical interpretation. In our experiments,  $s_1=0.99s_c$ ,  $s_2=1.01s_c$ ,  $\nu_1=0.99\nu_c$ , and  $\nu_2=1.01\nu_c$  gives a good performance.

## 4. Experimental results and performance analysis

In the following experiments, the ABC control parameters are set as: the number of nectar sources 40, the iteration limit of abandonment 80, and the maximum iteration number 2000.

### *4.1 Ultrasonic echo estimation for simulated ultrasonic NDE signals*

#### *4.1.1 Ultrasonic signal generation*

In this section, simulation experiments were carried out to quantitatively evaluate the performance of the proposed ABC-MP algorithm on ultrasonic echo estimation. Ultrasonic signals were created according to the ultrasonic signal model of Equation (3), where the incident pulses were simulated by the measured ultrasonic echoes from a standard steel test block in a water tank using 230, 100, 50, 30, and 20-MHz transducers respectively on a Sonoscan's D9000 system. The measured ultrasonic echoes are firstly normalized. Then, each echo  $s_i(t)$  in an ultrasonic signal was generated according to Equation (3), where the reflection coefficient that determined the amplitude of each echo, was changed to simulate different reflectivity properties of the interrogated defects/interfaces. Each echo was translated along the time axis to various time positions to simulate a wide diversity of interfaces at different depths. The simulated signal was the superposition of several echoes according to Eq. (3), and various signals are generated for test.

Notice that using the measure echoes rather than the ultrasonic echo model of Equation (1) to generate simulated ultrasonic signals makes the simulation as close to practice as

possible. It has been widely used in the community of ultrasonic NDE signal processing.

#### 4.1.2. Performance criteria

The performance of ABC-MP was measured quantitatively by four performance criteria: energy error, coefficient error, amplitude error, and the energy of the residue signal. The energy error  $E_{error}$  is defined as:

$$E_{error} = \frac{\|\tilde{s}_i - s_i\|_2}{\|s_i\|_2} \times 100\%, \quad (16)$$

where  $s_i$  is the original echo and  $\tilde{s}_i$  is the recovered echo. The coefficient error is defined as:

$$c_{error} = \frac{||\tilde{c}_i| - |c_i||}{|c_i|} \times 100\%, \quad (17)$$

where  $c_i$  is the original reflection coefficient, and  $\tilde{c}_i$  is the estimated reflection coefficient.

The amplitude error is defined as:

$$A_{error} = \frac{|\tilde{A}_i - A_i|}{|A_i|} \times 100\%, \quad (18)$$

where  $A_i$  is the peak intensity value of the original echo  $s_i$ , and  $\tilde{A}_i$  is the peak intensity value of the recovered echo  $\tilde{s}_i$ . The energy of the residue signal is defined as:

$$E_{residue} = \|R^{(m)}\|_2, \quad (19)$$

where  $R^{(m)}$  is the residue signal after decomposition.

From Section 1.1, it can be the four performance criteria are tightly related to the quality of ultrasonic echo estimation in practical ultrasonic NDE applications. They are good indicators for accuracy of defect detection and sizing. For example, the energy error  $E_{error}$  measures the overall quality, including the echo shape. The amplitude error measures accuracy of defect sizing. Moreover, in ultrasonic imaging, ultrasonic images are normally

generated by using the amplitude, as a result, the amplitude error is a direct measure of the image quality.

#### *4.1.3 Generation of discrete Gabor dictionary*

In the experimental tests, MP were carried out as well for the comparison purpose. To numerically implement the MP method, the first issue is to select a discrete subset in the continuous parameter space of  $(s, u, v, w)$ , i.e., to generate a discrete Gabor dictionary.

There are various sampling schemes to generate a discrete Gabor dictionary [30]. The discrete Gabor dictionary used widely in the literature is generated by the sampling scheme described in Section 1.3. The generation of this discrete dictionary is closely related to the frame theory used in the wavelet transform. The dictionary is succinct and complete from a mathematical point of view. However, it generally is unsuitable for decomposing ultrasonic signals comprised of time-localized echoes. For ultrasonic signal decomposition, time-localized Gabor atoms better match time-localized echoes, i.e., small values for the scale  $s$  are preferred. Moreover, it is desirable that the frequency range of the Gabor atoms in the dictionary matches the spectrum of the signal, and the discretization interval is independent of the scale  $s$  to achieve a uniformly high resolution. A small and constant discretization interval for the time shift is preferred to obtain the property of translation invariance for the decomposition. Therefore, based on this sampling scheme, an alternative dictionary can be generated for which the upper and lower bounds of the frequency  $v$ , scale  $s$ , and time shift  $u$  are determined as described in the Section 3.4 to give meaningful decomposition results for an ultrasonic signal. The bounds of the parameters  $\beta = (s, u, v, w)$  are the same with the

continuous parameter space of atoms used in ABC-MP. The superior performance of this sampling scheme has been demonstrated in [21, 31].

The second sampling scheme is used to generate a discrete Gabor dictionary for the MP decomposition in our experiments. The parameters  $\beta = (s, u, v, w)$  were discretized independently. The discretization interval is determined empirically to get the best performance of MP for fair comparison with ABC-MP.

#### *4.1.4 Results and analysis*

Figure 1(a) shows a simulated signal. Figure 1(b) shows the three composing echoes which were obtained by 100, 50, and 30-MHz transducers. Figure 2 shows the spectrum of each composing echo. Notice that the peak frequencies of these echoes are far less than the transducer frequencies due to the dispersive attenuation in water and packaging materials. The simulated signal was processed by the proposed ABC-MP approach, and the processed results are presented in Figure 3, Figure 3(a) shows the recovered echoes, while Figure 3(b) shows the reconstructed signal. Figure 3(c) displays the sparse representation in the phase plane, and Figure 3(d) is the residue signal.

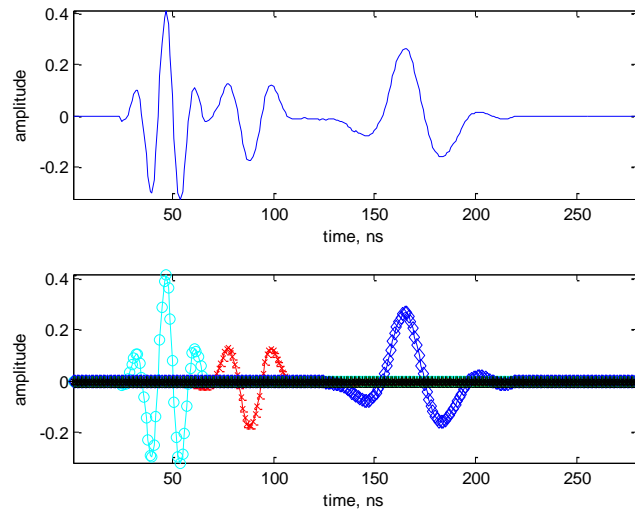


Figure 1: (a) The simulated signal; (b) The composing echoes.

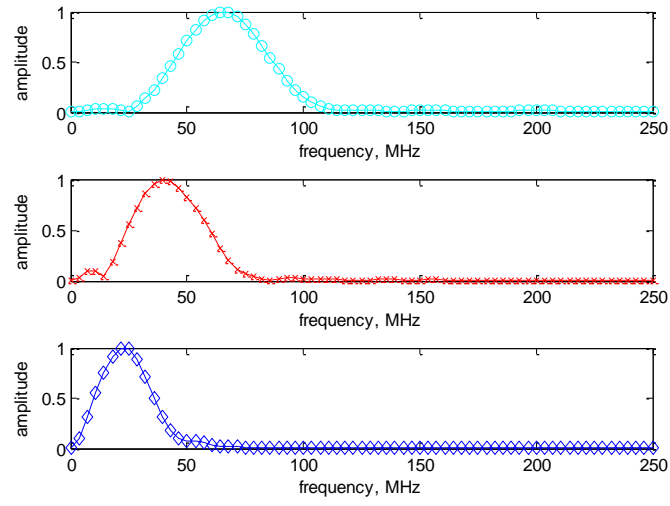


Figure 2: Spectrum of the composing echoes in Figure 1(b). Top to bottom: for the echoes from left to right in Figure 1(b) respectively.

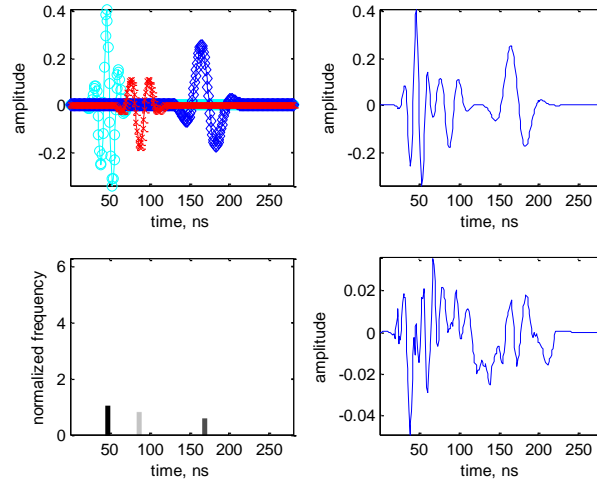


Figure 3: Processed results obtained by the proposed ABC-MP approach for the simulated signal shown in Figure 1(a). (a) The recovered composing echoes; (b) The reconstructed signal; (c) The sparse representation in the phase plane; (d) The residue.

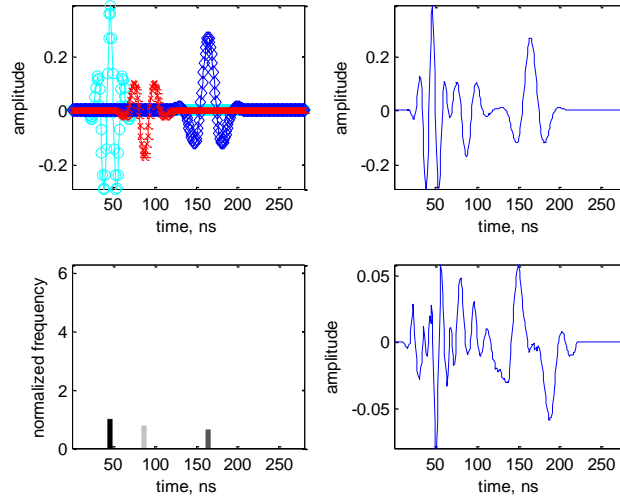


Figure 4: Processed results obtained by MP for the simulated signal shown in Figure 1(a). (a) The recovered composing echoes; (b) The reconstructed signal; (c) The sparse representation in the phase plane; (d) The residue.

For the purpose of comparison, the processed results obtained using MP and the discrete Gabor dictionary generated in Section 4.1.3, are presented in Figure 4. The quantitative

results from Figures 3 and 4 are presented in Table1.  $E_{residue}$  for the residue signals shown in Figures 3d and 4d are 12.05% and 21.85% respectively. From Figures 1b, 3a, and 4a, it can be seen that the accuracy of recovered echoes by the proposed ABC-MP approach are much higher than the MP method in terms of amplitude and shape. Comparing Figure 3(d) and Figure 4(d), it is also observed that the residue signal produced by ABC-MP is smaller than MP. The quantitative analysis results above confirm the superior performance of ABC-MP in ultrasonic echo estimation. Experimental verification were carried out over a large number of simulated signals, and very similar performance to the results presented here are observed.

In addition, the MP algorithm searches the optimal atom greedily in the Gabor dictionary which has 31360 atoms. Under the same conditions, the ABC algorithm searching the optimal atom, just needs to search 1000 space parameter points at most, i.e., the number of iterations to reach convergence is less than 1000. Thus, the proposed ABC-MP is much more efficient than MP in terms of computation time.

Table 1. The performance of ABC-MP.

	$E_{error}(\%)$		$c_{error}(\%)$		$A_{error}(\%)$	
	ABC-MP	MP	ABC-MP	MP	ABC-MP	MP
The first echo	11.52	17.19	0.88	1.79	1.69	5.84
The second echo	14.89	25.98	3.91	6.36	0.87	3.36
The third echo	10.94	26.14	0.52	3.45	1.93	5.07

#### ***4.2 Pulse detection and noise suppression for simulated ultrasonic NDE signals***



In this experiment, the performance of the proposed ABC-MP algorithm was tested by applying it for pulse detection and noise suppression. The pulse detection and noise suppression technique proposed in [31] is adapted by using the ABC-MP algorithm replacing the SBL algorithm. In particular, a noisy ultrasonic signal was firstly decomposed into sparse representations using the ABC-MP algorithm. Pulse detection and noise suppression was then carried out on the decomposed coefficients in the time-frequency domain. Nonlinear post-processing including thresholding and pruning was applied to the decomposed coefficients to reduce the noise contribution and extract the flaw information. Because of the high compact essence of sparse representations, flaw echoes are packed into a few significant coefficients, and noise energy is likely scattered all over the dictionary atoms, generating insignificant coefficients. This property greatly increases the efficiency of the pruning and thresholding operations, and is extremely useful for detecting flaw echoes embedded in background noise. Finally, reconstruct the ultrasonic signal using the processed coefficients and the corresponding dictionary atoms.

Computer generated white Gaussian noise was added to the simulated signal shown in Figure 1(a), and the resulting noisy signal was processed using the proposed technique. In order to quantify the efficiency of the proposed approach in ultrasonic signal detection, the output SNR was evaluated as a function of the input SNR. The output  $SNR_{out}$  is calculated as the ratio of the output signal power computed in a time window where the ultrasonic echoes are present and another time window for which the original echoes are null.  $SNR_{in}$  is calculated as the ratio of the power of the simulated signal shown in Figure 1(a) and the power of noise added to it. Figure 5 shows an example of our experimental results. The MP

decomposition was carried using the same way in Section 4.1. From Figure 5, it can be seen that the proposed ABC-MP algorithm outperforms MP.

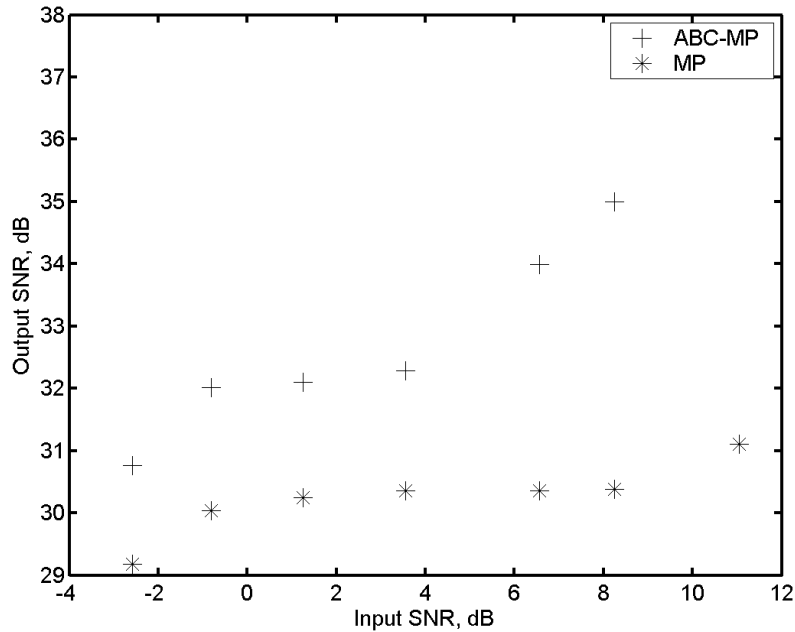


Figure 5: Input SNR versus output SNR

#### 4.3 Ultrasonic echo estimation for real ultrasonic NDE signals

In this experiment, the performance of the ABC-MP algorithm was tested using real ultrasonic NDE signals. Figure 6(a) shows a measured signal using a 100-MHz transducer on our commercial acoustic micro imaging system when inspecting a flip-chip package. The structure of a flip-chip package can be found from Ref.[32]. The measured signal contains three echoes. The first echo is the reflected echo from the interface of water-silicon die. The second echo is the reflected echo from the silicon die-solder joint. The second echo is reflected from a defect inside the solder joint. The spectrum of the signal is plotted in Figure 6(b). Figure 7 shows the processed results obtained using the proposed ABC-MP approach, and as a comparison, Figure 8 shows the processed results obtained using MP. Comparing

Figures 7 and 8, it can be seen that ABC-MP outperforms MP in terms of the shapes and amplitudes of the recovered echoes. Furthermore,  $E_{residue}$  for the residue signals shown in Figures 7 and 8 are 27.59% and 35.48% respectively. This further confirms the superior performance of ABC-MP.

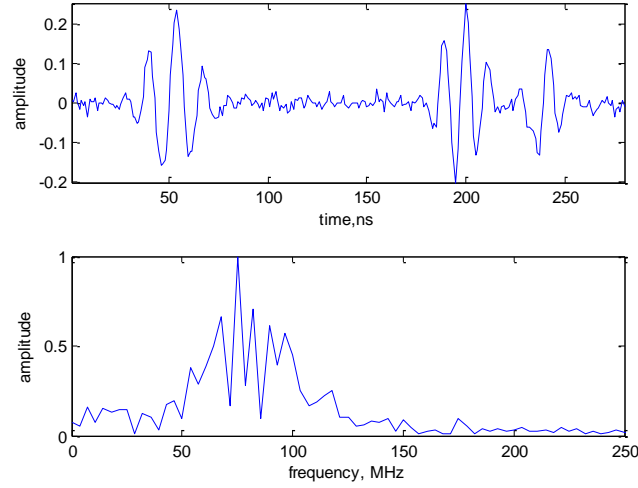


Figure 6: (a) A measured ultrasonic signal using a 100-MHz transducer and (b) its spectrum.

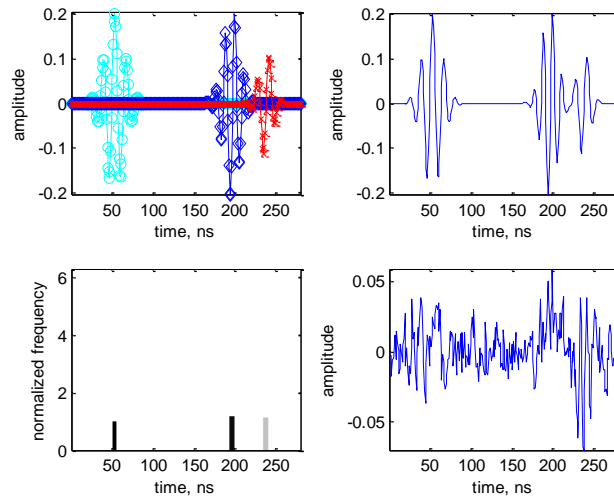


Figure 7: Processed results obtained by the proposed ABC-MP approach for the measured signal shown in Figure 6(a). (a) The recovered echoes; (b) The reconstructed signal; (c) The sparse representation in the phase plane; (d) The residue.

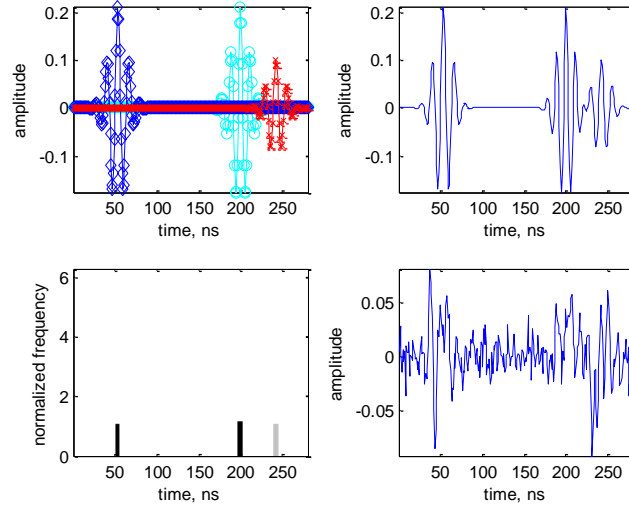


Figure 8: Processed results obtained by MP for the measured signal shown in Figure 6(a). (a) The recovered echoes; (b) The reconstructed signal; (c) The sparse representation in the phase plane; (d) The residue.

## 5 Conclusions

In this paper, an artificial bee colony optimization based matching pursuit approach for ultrasonic echo estimation is proposed. The signal is approximated by constructing a linear combination of atoms selected from the dictionary by ABC which finds the global optimal solution with quick convergence. Because ABC searches the optimal atoms in a continuous parameter space, it allows highly flexible of the adaptation of the approximation to the non-stationary nature of ultrasonic NDE signals. These advantages of ABC-MP lead to superior performance in ultrasonic echo estimation, pulse detection and noise suppression, which have been demonstrated from both simulated and measured signals.

## ACKNOWLEDGEMENTS

This work has been supported by the National Natural Science Foundation of China (No. 61674121, No.51705418).

## References

- [1] R. Demirli and J. Sanile, *Model-based estimation of ultrasonic echoes part I: analysis and algorithm*, IEEE Trans. Ultrason., Ferroelect., Freq. Contr., 48:787-802, 2001.
- [2] L. W. Schmerr, *Fundamentals of ultrasonic non-destructive evaluation: a modelling approach*, Plenum Press, New York, 1998.
- [3] G.-M. Zhang, David M. Harvey, “Contemporary ultrasonic signal processing approaches for nondestructive evaluation of multilayered structures,” *Nondestructive Testing & Evaluation*, 27(1):1-27, 2012.
- [4] G. Davis, S. Mallat, and M. Avellaneda, “Greedy adaptive approximation,” *J. Constr. Approx.*, 13:57-98, 1997.
- [5] P. S. Huggins and Steven W. Zucker, “Greedy basis pursuit,” *IEEE Trans. Signal Process.*, **55**:3760-3772, 2007.
- [6] D. P. Wipf and B. D. Rao, “Sparse Bayesian learning for basis selection,” *IEEE Trans Signal Process.*, 52:2153-2164, 2004.
- [7] I. Selesnick and M. Farshchian, “Sparse signal approximation via nonseparable regularization,” *IEEE Trans. Signal Processing*, 65(10): 2561-2575, 2017.
- [8] J. Hou, L.-P. Chau, Y. He, and P. A. Chou, “Sparse representation for colors of 3D point cloud via virtual adaptive sampling,” *IEEE International Conference on Acoustics*,

Speech and Signal Processing (ICASSP), 2017.

- [9] J. Yang, W. Su, and H. Gu, “High resolution multiple input multiple output inverse synthetic aperture radar imaging based on sparse representation,” *IET Radar, Sonar & Navigation*, 10(7): 1277 – 1285, 2016.
- [10] I. Fedorov, R. Giri, B.D. Rao, and T. Q. Nguyen, “Robust Bayesian method for simultaneous block sparse signal recovery with applications to face recognition,” *IEEE International Conference on Image Processing (ICIP)*, 2016.
- [11] Y. Yang and S. Nagarajaiah, “Structural damage identification via a combination of blind feature extraction and sparse representation classification,” *Mechanical Systems and Signal Processing*, 45(1):1-23, 2014.
- [12] W. Fan, G. Cai, Z.K. Zhu, C. Shen, W. Huang, and L. Shang, “Sparse representation of transients in wavelet basis and its application in gearbox fault feature extraction,” *Mechanical Systems and Signal Processing*, 56–57: 230-245, 2015.
- [13] M. S. Lewicki and T. J. Sejnowski, “Learning overcomplete representations,” *Neural Computation*, **12**:337-365, 2000.
- [14] S. S. Chen, D. L. Donoho, and M.A. Saunders, “Atomic decomposition by basis pursuit,” *SIAM J. Sci. Comput.*, **20**:33-61, 1999.
- [15] R. Coifman and D. L. Donoho, “Translation invariant de-noising,” *Wavelets and Statistics*, Lecture Notes in Statistics \_Springer-Verlag, New York, , pp. 125–150, 1995.
- [16] C. Xu, P. Zhang, H. Wang, Y. Li, and C. Lv, “Ultrasonic echo waveshape features extraction based on QPSO-matching pursuit for online wear debris discrimination,” *Mechanical Systems and Signal Processing*, 60–61: 301-315, 2015.

- [17] B. Wu, Y. Huang, X. Chen, S. Krishnaswamy, and H. Li, "Guided-wave signal processing by the sparse Bayesian learning approach employing Gabor pulse model," *Structural Health Monitoring*, 16(3): 347-362, 2017.
- [18] B. Wu, Y. Huang, and S. Krishnaswamy, "A Bayesian approach for sparse flaw detection from noisy signals for ultrasonic NDT," *NDT & E International*, 85:76-85, 2017.
- [19] G.-M. Zhang, D.M. Harvey, D.R. Burton, "Micro non-destructive evaluation of microelectronics using three dimension acoustic imaging," *Applied Physics Letters*, 98:094102, 3pages, 2011.
- [20] Y. Lu and J. E. Michaels, "Numerical implementation of matching pursuit for the analysis of complex ultrasonic signals," *IEEE transactions on ultrasonics, ferroelectrics, and frequency control*, 55(1):173-181, 2008
- [21] G-M. Zhang and D.M. Harvey, "Sparse Signal Representation and its Applications in Ultrasonic NDE," *Ultrasonics*, 52(3):351-363, 2012.
- [22] J. A. Trop, "Greed is good: algorithmic results for sparse approximation," *IEEE Trans. Information Theory*, 50:2231-2242, 2004.
- [23] S.E. Ferrando, L.A. Kolasa, and N. Kovacevic, "A flexible implementation of matching pursuit for Gabor dictionaries," *ACM Trans. Mathematical Software*, 28(3):337-353, 2002.
- [24] S.G. Mallat and Z. Zhang, 'Matching pursuit with time-frequency dictionaries', *IEEE Trans. On Signal Processing*, 41(12): 3397-3415, 1993.
- [25] J. Kennedy and R. Eberhart, "Particle swarm optimization". *Proceedings of IEEE International Conference on Neural Networks*, IV, pp. 1942–1948, 1995.

- [26] S. Kirkpatrick, C. D. Gelatt, and M. P. Vecchi, "Optimization by simulated annealing," *Science, New Series*, 220(4598): 671-680, 1983.
- [27] D. Karaboga and B. Akay, "A modified artificial bee colony (ABC) algorithm for constrained optimization problems," *Applied Soft Computing*, 11:3021-3031, 2011.
- [28] D. Karaboga and C. Ozturk, "A novel clustering approach: artificial bee colony algorithm," *Applied Soft Computing*, 11:652-657, 2011.
- [29] D. Karaboga and B. Basturk, "On the performance of artificial bee colony (ABC) algorithm," *Applied Soft Computing*, 8:687-697, 2008.
- [30] H.G. Feichtinger and T. Strohmer, Eds., *Gabor analysis and algorithms, theory and application*. Cambridge, MA: Birkhauser, 1998.
- [31] G.-M. Zhang, D. M. Harvey, and D. R. Braden, "Signal denoising and ultrasonic flaw detection via overcomplete and sparse representations," *J. Acoust. Soc. Am.*, 124(5):2963-2972, 2008.
- [32] C. S. Lee, G.-M. Zhang, D. M. Harvey, and A. Qi, "Characterization of micro-crack propagation through analysis of edge effect in acoustic microimaging of microelectronic packages", *NDT & E International*, 79: 1–6, 2016.